
Functional optimal transport: map estimation and domain adaptation for functional data

Jiacheng Zhu*
Carnegie Mellon University
jzhu4@andrew.cmu.edu

Aritra Guha*
Duke University
aritra.guha@duke.edu

Dat Do*
University of Michigan
dodat@umich.edu

Mengdi Xu
Carnegie Mellon University
mengdixu@andrew.cmu.edu

Xuanlong Nguyen
University of Michigan
xuanlong@umich.edu

Ding Zhao
Carnegie Mellon University
dingzhao@cmu.edu

Abstract

We introduce a formulation of optimal transport problem for distributions on function spaces, where the stochastic map between functional domains can be partially represented in terms of an (infinite-dimensional) Hilbert-Schmidt operator mapping a Hilbert space of functions to another. For numerous machine learning tasks, data can be naturally viewed as samples drawn from spaces of functions, such as curves and surfaces, in high dimensions. Optimal transport for functional data analysis provides a useful framework of treatment for such domains. In this work, we develop an efficient algorithm for finding the stochastic transport map between functional domains and provide theoretical guarantees on the existence, uniqueness, and consistency of our estimate for the Hilbert-Schmidt operator. We validate our method on synthetic datasets and study the geometric properties of the transport map. Experiments on real-world datasets of robot arm trajectories further demonstrate the effectiveness of our method on applications in domain adaptation.

1 Introduction

Optimal transport (OT) is a formalism for finding and quantifying the movement of mass from one probability distribution to another [48]. In recent years, it has been instrumental in various machine learning tasks, including deep generative modeling [3, 42], unsupervised learning [19, 33] and domain adaptations [15, 4]. As statistical machine learning algorithms are applied to increasingly complex domains, it is of interest to develop optimal transport based methods for complex data structures. A particularly common form of such structures arises from functional data — data that may be viewed as random samples of smooth functions, curves or surfaces in high dimension spaces [37, 21, 11]. Examples of real-world machine learning applications involving functional data are numerous, ranging from robotics [9] and natural language processing [41] to economics [20] and healthcare [6]. It is natural to take a *functional optimal transport* approach in such domains.

The goal of this paper is to provide a novel formulation of the optimal transport problem in function spaces, to develop an efficient learning algorithm for estimating a suitable notion of optimal stochastic map that transports samples from one functional domain to another, to provide theoretical guarantees regarding the *existence*, *uniqueness* and *consistency* of our estimates, and to demonstrate the effectiveness of our approach to several application domains where the functional optimal transport

*Equal contribution

viewpoint proves natural and useful. There are several formidable challenges: both the source and the target function spaces can be quite complex, and in general of infinite dimensions. Moreover, one needs to deal with the distributions over such spaces, which is difficult if one is to model them. In general, the optimal coupling or the underlying optimal transport map between the two distributions is hard to characterize and compute efficiently. Yet, to be useful one must find an explicit transport map that can approximate well the optimal coupling (the original Monge problem) [48, 38].

There is indeed a growing interest in finding an explicit optimal transport map linked to the Monge problem. For discrete distributions, map estimation can be tackled by jointly learning the coupling and a transformation map [38]. This basic idea and extensions were shown to be useful for the alignment of multimodal distributions [29] and word embedding [54, 18]; such joint optimization objective was shown [1] to be related to the softassign Procrustes method [40]. Meanwhile, a different strand of work focused on scaling up the computation of the transport map [17, 36], including approximating transport maps with neural networks [43, 32], deep generative models [51], and flow models [22]. Most existing approaches learn a map that transports point mass from one (empirical) distribution to another. To the best of our knowledge, there is scarcely any work that addresses optimal transport in the domains of functions by specifically accounting for the functional data structure. A naive approach to functional data is to treat a function as a vector of components sampled at a number of design points in its domain. Such an approach fails to exploit the fine structures (e.g., continuity, regularity) present naturally in many functional domains and would be highly sensitive to the choice of design points as one moves from one domain to another.

The mathematical machinery of functional data analysis (FDA) [21], along with recent advances in computational optimal transport via regularization techniques will be brought to bear on the aforementioned problems. First, we take a model-free approach, by avoiding making assumptions on the source and target distributions of functional data. Instead, we aim for learning the (stochastic) transport map directly. Second, we follow the FDA perspective by assuming that both the source and target distributions be supported on suitable Hilbert spaces of functions H_1 and H_2 , respectively. A map $T : H_1 \rightarrow H_2$ sending elements of H_1 to that of H_2 will be represented by a class of linear operators, namely the integral operators. In fact, we shall restrict ourselves to Hilbert-Schmidt operators, which are compact, and computationally convenient to regularize and amenable to theoretical analysis. Finally, the optimal *deterministic* transport map between two probability measures on function spaces may not exist; the characterization of existence and uniqueness for the deterministic map remains unknown. To get around this, we enlarge the space of transport maps by allowing for stochastic coupling Π between the two domains $T(H_1) \subseteq H_2$ and H_2 , while controlling the complexity of such coupling via the entropic regularization technique initiated by [8].

This formulation has two complementary interpretations: it can be viewed as learning an integral operator regularized by a transport plan (a coupling distribution) or it can also be seen as an optimal coupling problem (the Kantorovich problem), which is associated with a cost matrix parametrized by the integral operator. In any case, we take a joint optimization approach for the transport map T and the coupling distribution Π in functional domains. Subject to suitable regularizations, the existence of optimal (T, Π) and uniqueness for T can be established, which leads to a consistency result of our estimation procedure (Section 3). Our estimation procedure involves solving a block coordinate-wise convex optimization, and admits an efficient algorithm for finding explicit transport map that can be applied on sampled functions, as described in Section 4. In Section 5, the effectiveness of our approach is validated first on synthetic datasets of smooth functional data and then applied in a suite of experiments mapping real-world 3D trajectories between robotic arms with different configurations. Code is available here: <https://github.com/VersElectronics/FOT>

2 Preliminaries

This section provides some basic background of optimal transport and functional data analysis.

Optimal transport The basic problem in optimal transport, the so-called Kantorovich problem [48, 25], is to find an optimal coupling π of given measures $\mu \in \mathcal{M}(\mathcal{X})$, $\nu \in \mathcal{M}(\mathcal{Y})$ to minimize

$$\inf_{\pi \in \Pi} \int_{\mathcal{X} \times \mathcal{Y}} c(x, y) d\pi(x, y), \text{ subject to } \Pi = \{\pi : \gamma_{\#}^{\mathcal{X}} \pi = \mu, \gamma_{\#}^{\mathcal{Y}} \pi = \nu\}. \quad (1)$$

In the above display, $c : \mathcal{X} \times \mathcal{Y} \mapsto \mathbb{R}^+$ is a cost function and $\gamma^{\mathcal{X}}, \gamma^{\mathcal{Y}}$ denote projections from $\mathcal{X} \times \mathcal{Y}$ onto \mathcal{X} and \mathcal{Y} respectively, while $T_{\#}\pi$ generally denotes the pushforward measure of π by a map T . This optimization is well-defined and the optimal π exists under mild conditions (in particular, \mathcal{X}, \mathcal{Y} are both separable and complete metric spaces, c is lower semicontinuous) [48]. When $\mathcal{X} = \mathcal{Y}$ are metric spaces, $c(x, y)$ is the square of the distance between x and y , then the square root of the optimal cost given by (1) defines the Wasserstein metric $W_2(\mu, \nu)$ on $\mathcal{M}(\mathcal{X})$. A related problem is Monge problem, where one finds a Borel map $T : \mathcal{X} \rightarrow \mathcal{Y}$ that realizes the infimum

$$\inf_T \int_{\mathcal{X}} c(x, T(x)) d\mu(x) \quad \text{subject to } T_{\#}\mu = \nu. \quad (2)$$

Note that the existence of the optimal deterministic map T is not always guaranteed [48]. However, in various applications, it is of interest to find a deterministic map that approximates the optimal coupling to the Kantorovich problem. In many recent work, it is shown naturally to restrict T in a family of maps \mathcal{F} and optimize T and π jointly [38, 1, 18, 43, 2]:

$$\inf_{\pi \in \Pi, T \in \mathcal{F}} \int_{\mathcal{X} \times \mathcal{Y}} c(T(x), y) d\pi(x, y), \quad (3)$$

where $c : \mathcal{Y} \times \mathcal{Y} \mapsto \mathbb{R}^+$ is a cost function on \mathcal{Y} . The family \mathcal{F} is often chosen to be meaningful depending on the spaces \mathcal{X}, \mathcal{Y} and measures μ, ν . For instance, \mathcal{F} may be a class of linear functions (e.g. rigid transformations) [38, 2] or neural networks [43].

At a high level, our approach will be analogous to (3), except that \mathcal{X} and \mathcal{Y} are taken to be Hilbert spaces of functions, as we are motivated by applications in functional domains (see Fig. 1 for an illustration). Thus we will be working with distributions on Hilbert spaces of functions, while \mathcal{F} is a suitable class of operators. This leads us to the framework of functional data analysis.

Functional data analysis adopts the perspective that certain types of data may be viewed as samples of random functions, which are taken as random elements taking value in Hilbert spaces of functions. Thus, data analysis techniques on functional data involve operations acting on Hilbert spaces. Let $A : H_1 \rightarrow H_2$ be a bounded linear operator, where H_1 (respectively, H_2) is a Hilbert space equipped with scalar product $\langle \cdot, \cdot \rangle_{H_1}$ (respectively, $\langle \cdot, \cdot \rangle_{H_2}$) and $(U_i)_{i \geq 1} ((V_j)_{j \geq 1})$ is the Hilbert basis in H_1 (H_2). We will focus on a class of compact integral operators, namely Hilbert-Schmidt operators, that are sufficiently rich for many applications and yet amenable to analysis and computation. A is said to be Hilbert-Schmidt if $\sum_{i \geq 1} \|AU_i\|_{H_2}^2 < \infty$ for any Hilbert basis $(U_i)_{i \geq 1}$. The space of Hilbert-Schmidt operators between H_1 and H_2 , to be denoted by $\mathcal{B}_{HS}(H_1, H_2)$, is also a Hilbert space endowed with the scalar product $\langle A, B \rangle_{HS} = \sum_i \langle AU_i, BU_i \rangle_{H_2}$ and the corresponding Hilbert-Schmidt norm is denoted by $\|\cdot\|_{HS}$.

Recall that the outer product operator between two elements $e_i \in H_i$ for $i = 1, 2$ is denoted by $e_1 \otimes_1 e_2 : H_1 \rightarrow H_2$ and is defined by $(e_1 \otimes_1 e_2)f = \langle e_1, f \rangle_{H_1} e_2$ for $f \in H_1$. An important fact of Hilbert-Schmidt operators is given as follows (cf. Theorem 4.4.5 of [21]).

Theorem 1. *The linear space $\mathcal{B}_{HS}(H_1, H_2)$ is a separable Hilbert space when equipped with the HS inner product. For any choice of complete orthonormal basis system (CONS) $\{U_i\}$ and $\{V_j\}$ for H_1 and H_2 respectively, $\{U_i \otimes_1 V_j\}$ forms a CONS for $\mathcal{B}_{HS}(H_1, H_2)$.*

As a result, the following representation of Hilbert-Schmidt operators and their norm will be useful.

Lemma 1. *Let $\{U_i\}_{i=1}^{\infty}, \{V_j\}_{j=1}^{\infty}$ be a CONS for H_1, H_2 , respectively. Then any Hilbert-Schmidt operator $T \in \mathcal{B}_{HS}(H_1, H_2)$ can be decomposed as*

$$T = \sum_{i,j} \lambda_{ij} U_i \otimes_1 V_j, \quad \text{where } \|T\|_{HS}^2 = \sum_{i,j} \lambda_{ij}^2. \quad (4)$$

3 Functional optimal transport: optimization and convergence analysis

We are ready to devise a functional optimal transport formulation based on the framework of Hilbert-Schmidt operators and characterize the existence, uniqueness and consistency of our proposed estimators, given sampled functions from source and target domains.

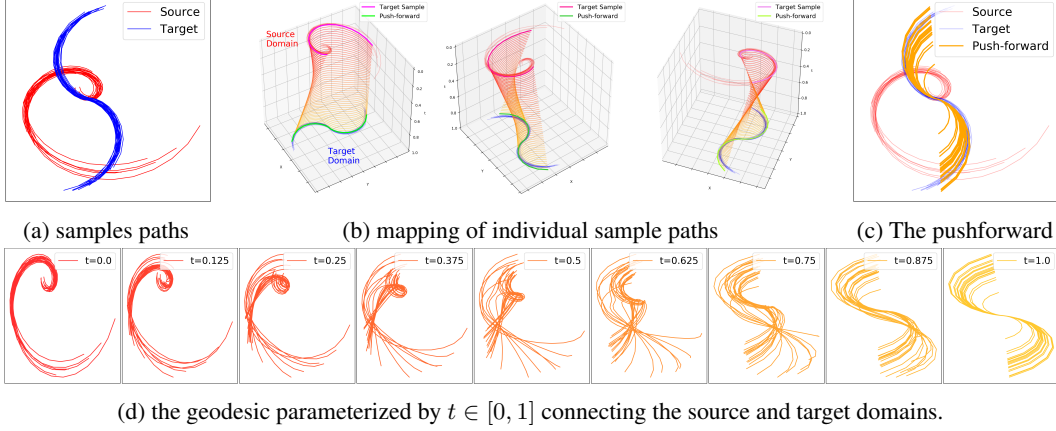


Figure 1: Illustration of the estimated pushforward maps that send sample paths from the source **Swiss-roll curve dataset** to the target **Wave curve dataset** domain. (a) Datasets are a collection of continuous sample paths. (b) Three individual samples are mapped from source to target. (c) Pushforward applied to all samples. (d) The resulting geodesic between source and target.

Given Hilbert spaces of function H_1 and H_2 , which are endowed with Borel probability measures μ and ν , respectively, we wish to find a Borel map $\Gamma : H_1 \mapsto H_2$ such that ν is the pushforward measure of μ by Γ . Expressing this statement probabilistically, if $f \sim \mu$ represents a random element of H_1 , then Γf is a random element of H_2 and $\Gamma f \sim \nu$. As noted in Section 2, such a map may not always exist, but this motivates the following formulation:

$$\Gamma := \arg \inf_{T \in \mathcal{B}_{HS}(H_1, H_2)} W_2(T\#\mu, \nu), \quad (5)$$

where $T\#\mu$ is the pushforward of μ by T , and W_2 is the Wasserstein distance of probability measures on H_2 . The space of solutions of Eq. (5) may still be large and the problem itself might be ill-posed; thus we consider imposing a shrinkage penalty, which leads to the problem of finding the infimum of the following objective function $J : \mathcal{B}_{HS} \rightarrow \mathbb{R}_+$:

$$\inf_{T \in \mathcal{B}_{HS}} J(T), \quad J(T) := W_2^2(T\#\mu, \nu) + \eta \|T\|_{HS}^2, \quad (6)$$

where $\eta > 0$. It is natural to study the objective function J and ask if it has a unique minimizer. To characterize this problem, we put a mild condition on the moments of μ and ν , which are typically assumed for probability measures on Hilbert spaces [30]. We shall assume throughout the paper that

$$E_{f_1 \sim \mu} \|f_1\|_{H_1}^2 < \infty, \quad E_{f_2 \sim \nu} \|f_2\|_{H_2}^2 < \infty. \quad (7)$$

Key properties of objective function (6) are as follows (all proofs are given in Appendix A).

Lemma 2. *The following statements hold.*

- (i) $W_2(T\#\mu, \nu)$ is a Lipschitz continuous function of $T \in \mathcal{B}_{HS}(H_1, H_2)$, which implies that $J : \mathcal{B}_{HS}(H_1, H_2) \rightarrow \mathbb{R}_+$ is also continuous.
- (ii) J is a strictly convex function.
- (iii) There are constants $C_1, C_2 > 0$ such that $J(T) \leq C_1 \|T\|^2 + C_2 \quad \forall T \in \mathcal{B}_{HS}(H_1, H_2)$.
- (iv) $\lim_{\|T\| \rightarrow \infty} J(T) = \infty$.

Thanks to Lemma 2, the existence and uniqueness properties can be established.

Theorem 2. *There exists a unique minimizer T_0 for problem (6).*

The challenge of solving (6) is that this is an optimization problem in the infinite dimensional space of operators \mathcal{B}_{HS} . To alleviate this complexity, we reduce the problem to a suitable finite dimensional approximation. We follow techniques in numerical functional analysis by taking a finite number of basis functions.

In particular, for some finite K_1, K_2 , let $B_K = \text{Span}(\{U_i \otimes V_j : i = \overline{1, K_1}, j = \overline{1, K_2}\})$, where $K = (K_1, K_2)$. This yields the optimization problem of $J(T)$ over the space $T \in B_K$. The following result validates the choice of approximate optimization.

Lemma 3. *For each $K = (K_1, K_2)$, there exists a unique minimizer T_K of J over B_K . Moreover, $T_K \rightarrow T_0$ as $K_1, K_2 \rightarrow \infty$.*

Consistency of M-estimator In practice, we are given i.i.d. samples $f_{11}, f_{12}, \dots, f_{1n_1}$ from μ and $f_{21}, f_{22}, \dots, f_{2n_2}$ from ν , the empirical version of our optimization problem becomes:

$$\inf_{T \in \mathcal{B}_{HS}} \hat{J}_n(T), \quad \hat{J}_n(T) := W_2^2(T_{\#} \hat{\mu}_{n_1}, \hat{\nu}_{n_2}) + \eta \|T\|_{HS}^2, \quad (8)$$

where $\hat{\mu}_{n_1} = \frac{1}{n_1} \sum_{l=1}^{n_1} \delta_{f_{1l}}$ and $\hat{\nu}_{n_2} = \frac{1}{n_2} \sum_{k=1}^{n_2} \delta_{f_{2k}}$ are the empirical measures, and $n = (n_1, n_2)$.

We proceed to show that the minimizer of this problem exists and provides a consistent estimate of the minimizer of (6). The common technique to establish consistency of M-estimators is via the uniform convergence of objective functions \hat{J}_n to J . Since $\mathcal{B}_{HS}(H_1, H_2)$ is unbounded and locally non-compact, care must be taken to ensure that the minimizer of (8) is eventually bounded so that a suitable uniform convergence behavior can be established, as explicated in the following key lemma:

Lemma 4. 1. *For any fixed $C_0 > 0$,*

$$\sup_{\|T\| \leq C_0} |\hat{J}_n(T) - J(T)| \xrightarrow{P} 0 \quad (n \rightarrow \infty). \quad (9)$$

2. *For any n, K , \hat{J}_n has a unique minimizer $\hat{T}_{K,n}$ over B_K . Moreover, there exists a finite constant D such that $P(\sup_K \|\hat{T}_{K,n}\| < D) \rightarrow 1$ as $n \rightarrow \infty$.*

Building upon the above results, we can establish consistency of our M -estimator when there are enough samples and the dimensions K_1, K_2 are allowed to grow with the sample size:

Theorem 3. *The minimizer of Eq. (8) for $\hat{T}_{K,n} \in B_K$ is a consistent estimate for the minimizer of Eq. (6). Specifically, $\hat{T}_{K,n} \xrightarrow{P} T_0$ as $K_1, K_2, n_1, n_2 \rightarrow \infty$.*

It is worth emphasizing that the consistency of estimate $\hat{T}_{K,n}$ is ensured as long as sample sizes and approximate dimensions are allowed to grow. The specific schedule at which K_1, K_2 grow relatively to n_1, n_2 will determine the rate of convergence to T_0 , which is also dependent on the choice of regularization parameter $\eta > 0$, the true probability measures μ, ν , and the choice of CONS. It is of great interest to have a refined understanding on this matter. In practice, we can choose K_1, K_2 by a simple cross-validation technique, which we shall discuss further in the sequel.

4 Methodology and computational algorithm

Lemma 3 in the last section paves the way for us to find an approximate solution to the original fully continuous infinite-dimensional problem, by utilizing finite sets of basis function, in the spirit of Galerkin method [14], which is justified by the consistency theorem (Theorem 3). Thus, we can focus on solving the objective function (8) instead of (6).

Choosing a basis $\{U_i\}_{i=1}^{\infty}$ of H_1 and a basis $\{V_j\}_{j=1}^{\infty}$ of H_2 , and fixing K_1, K_2 , we want to find T based on the $K_1 \times K_2$ dimensional subspace of $\mathcal{B}_{HS}(H_1, H_2)$ with the basis $\{U_i \otimes V_j\}_{i=1, K_1, j=1, K_2}$. Lemma 1 gives us the following formula for T and its norm

$$T = \sum_{i=1}^{K_1} \sum_{j=1}^{K_2} \lambda_{ji} U_i \otimes V_j, \quad \|T\|_{HS}^2 = \sum_{i=1}^{K_1} \sum_{j=1}^{K_2} \lambda_{ji}^2. \quad (10)$$

As T is represented by matrix $\mathbf{\Lambda} = (\lambda_{ji})_{j,i=1}^{K_2, K_1}$, the cost to move function f_{1l} in H_1 to f_{2k} in H_2 is

$$\|T f_{1l} - f_{2k}\|^2 = \left\| \sum_{i=1}^{K_1} \sum_{j=1}^{K_2} \lambda_{ji} V_j \langle f_{1l}, U_i \rangle_{H_1} - f_{2k} \right\|_{H_2}^2 =: C_{lk}(\mathbf{\Lambda}). \quad (11)$$

Algorithm 1: Joint Learning of Λ and π

Input: Observed functional data $\{f_{1l} = (\mathbf{x}_{1l}, \mathbf{y}_{1l})\}_{l=1}^{n_1}$ and $\{f_{2k} = (\mathbf{x}_{2k}, \mathbf{y}_{2k})\}_{k=1}^{n_2}$, coefficient γ_h, γ_p, η , and learning rate l_r , source and target CONS $\{U_i(\cdot)\}_{i=1}^{K_1}$ and $\{V_j(\cdot)\}_{j=1}^{K_2}$.
Initial value $\Lambda_0 \leftarrow \Lambda_{ini}, \pi_0 \leftarrow \pi_{ini}$.
 $\mathbf{U}_{1l} = [U_1(\mathbf{x}_{1l}), \dots, U_{K_1}(\mathbf{x}_{1l})], \mathbf{V}_{2k} = [V_1(\mathbf{x}_{2k}), \dots, V_{K_2}(\mathbf{x}_{2k})]$ # Evaluate eigenfunctions
for $t = 1$ **to** T_{\max} **do**
 # Step 1. Update π_{t-1}
 $C_{lk} \leftarrow \|\mathbf{V}_{2k} \Lambda_t \mathbf{U}_{1l}^T \mathbf{y}_{1l} - \mathbf{y}_{2k}\|_F^2$ # Cost matrix by Eq.(14)
 $\pi_t \leftarrow \text{Sinkhorn}(\gamma_h, \mathbf{C})$ **OR** $\pi_t \leftarrow \text{argmin}_{\pi} \mathcal{L}(\pi, \lambda; \rho)$ # Sinkhorn or Lagrange multipliers
 # Step 2. Update Λ_{t-1} with gradient descent
 Learn Λ_t , solve Eq. (13) with fixed π_t using gradient descent
end for
Output: $\pi_{T_{\max}}, \Lambda_{T_{\max}}$

Hence, the optimization problem (8) as restricted to B_K can be written as

$$\min_{T \in B_K} \hat{J}_n(T) = \min_{\Lambda \in \mathbb{R}^{K_2 \times K_1}, \pi \in \hat{\Pi}} \sum_{l,k=1}^{n_1, n_2} \pi_{lk} C_{lk}(\Lambda) + \eta \|\Lambda\|_F^2. \quad (12)$$

where $\|\cdot\|_F$ is the Frobenius norm, and the empirical joint measure $\hat{\Pi} := \{\pi \in (\mathbb{R}^+)^{n_1 \times n_2} \mid \pi \mathbf{1}_{n_2} = \mathbf{1}_{n_1}/n_1, \pi^T \mathbf{1}_{n_1} = \mathbf{1}_{n_2}/n_2\}$ with $\mathbf{1}_n$ a length n vector of ones. Eq.(12) indicates we need to simultaneously learn the HS operator T and the joint distribution (coupling) π . Additionally, we also want to (i) use an entropic penalty to improve the computational efficiency [8], (ii) impose an l_p penalty on the coupling matrix via the term $\gamma_p \sum_{l,k=1}^{n_1, n_2} \pi_{lk}^p$, where $p \geq 1$. It ensures that the optimal coupling (π_{lk}) has fewer active parameters thereby easing computing for large datasets. Also this can be considered as imposing a robustness in addition to shrinkage, similar behavior is observed for the Huber loss [23]. The final objective function is

$$\arg \min_{\Lambda \in \mathbb{R}^{K_2 \times K_1}, \pi \in \hat{\Pi}} \sum_{l,k=1}^{n_1, n_2} C_{lk}(\Lambda) \pi_{lk} + \eta \|\Lambda\|_F^2 + \gamma_h \sum_{l,k=1}^{n_1, n_2} \pi_{lk} \log \pi_{lk} + \gamma_p \sum_{l,k=1}^{n_1, n_2} \pi_{lk}^p \quad (13)$$

where η, γ_h , and γ_p are the regularization coefficients.

Discretization via design points. For real data, we do not directly observe functions $(f_{1l})_{l=1}^{n_1}$ and $(f_{2k})_{k=1}^{n_2}$ but only their values $(\mathbf{y}_{1l})_{l=1}^{n_1}$ and $(\mathbf{y}_{2k})_{k=1}^{n_2}$ at design points $(\mathbf{x}_{1l})_{l=1}^{n_1}$ and $(\mathbf{x}_{2k})_{k=1}^{n_2}$, respectively, where $\mathbf{x}_{1l}, \mathbf{y}_{1l} \in \mathbb{R}^{d_{1l}}, \mathbf{x}_{2k}, \mathbf{y}_{2k} \in \mathbb{R}^{d_{2k}} \forall l, k$. The transportation cost C_{lk} becomes

$$C_{lk}(\Lambda) = \|\mathbf{V}_{2k} \Lambda \mathbf{U}_{1l}^T \mathbf{y}_{1l} - \mathbf{y}_{2k}\|_2^2, \quad (14)$$

where $\mathbf{U}_{1l} = [U_1(\mathbf{x}_{1l}), \dots, U_{K_1}(\mathbf{x}_{1l})] \in \mathbb{R}^{d_{1l} \times K_1}, \mathbf{V}_{2k} = [V_1(\mathbf{x}_{2k}), \dots, V_{K_2}(\mathbf{x}_{2k})] \in \mathbb{R}^{d_{2l} \times K_2}$. The objective function (12) can be computed accordingly. It is worth-noting that our method works even in the case where we observe our functions at different design points (and different numbers of design points). It is obvious that one *cannot* treat each function as a multidimensional vector to apply existing multivariate OT techniques in this case due to the dimensions mismatch.

Choosing basis functions and hyper-parameters. We can choose $\{U_i\}$ and $\{V_j\}$ based on the Karhunen-Loeve basis of a user-specified kernel. For example, radial kernels $k(x, z) = \exp(-\frac{\|x-z\|^2}{2l^2})$ corresponds to eigenfunctions [55] $e_j(x) \propto \exp-(b-a)x^2 H_j(x\sqrt{2c})$ where a, b , and c are coefficients related to kernel parameters and H_j is the j -th order Hermite polynomial. More choices of Karhunen-Loeve bases and their properties are described in Appendix C. It can be seen that increasing K_1 and K_2 can lower the objective function, but it can also hurt the generalization of the method as we only observe a finite number of sampled functions. We recommend using cross-validation to choose K_1, K_2 and regularization hyper-parameters η, γ_h, γ_p .

Optimization. The problem (12) is convex in Λ and π , separately. Therefore, we propose a coordinate-wise gradient descent approach to minimize the above function. The algorithm is described in Algorithm 1 and the explicit calculations are shown in Appendix B. Experimental results for various settings with this algorithm are described in the following section.

5 Experiments

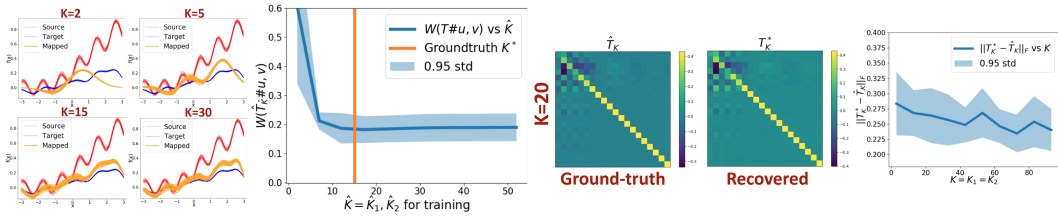


Figure 2: Left: As \hat{K} increases, $T_{\hat{K}}\#f_1$ moves toward f_2 and $W(T_{\hat{K}}\#\hat{u}, \hat{v})$ decreases until $\hat{K} \geq K^*$. Right: \hat{T}_K approximates T_K^* well, i.e., $\|T_K^* - \hat{T}_K\|_F$ keeps decreasing as K increases.

5.1 Simulation studies on synthetic continuous functional dataset

Verification of theory First, we present simulation studies to demonstrate that one can recover the "true" pushforward map via cross-validation. The result is described in Fig. 2, which illustrates the effects of varying the number of basis eigenfunctions $\hat{K} = (\hat{K}_1, \hat{K}_2)$. We explicitly constructed a ground-truth map T_0 that has finite intrinsic dimensions $K_1^* = K_2^* = 15$. Then we obtained the target curves by pushing forward source curves via T_0 . The FOT algorithm is then applied to the data while \hat{K}_1 and \hat{K}_2 gradually being increased. We observed that the performance of the estimated map got better as \hat{K} increased until it exceeded K^* . Further increasing the number of eigenfunctions did not reduce the learning objective.

We also directly validate Lemma 3 by evaluating $\hat{T}_{\hat{K}}$ from an infinite-dimensional map that transports sinusoidal functions. The Frobenius norm between the optimal T_K^* and estimated \hat{T}_K , $\|T_K^* - \hat{T}_K\|_F$, decreased as we increased K . In both simulations, we set sample sizes $n_1 = n_2 = 30$. For hyperparameters, set $\gamma_h = 20$, $\eta = 1$. It is noted that the results were quite robust to other choices of hyperparameter. More experimental settings can be found in Appendix C.

Baseline comparison We compared our method with several existing map estimation methods on synthetic *mixture of sinusoidal functions* dataset. Sample paths were drawn from sinusoidal functions with random parameters. Then, curves were evaluated on random index sets.

Details of this continuous dataset are given in Appendix C. In Fig. 3, FOT is compared against the following baselines: (i) Transport map of Gaussian processes [33, 35] where a closed form optimal transport map is available, (ii) Large-scale optimal transport (LSOT) [43], and (iii) Mapping estimation for discrete OT (DSOT) [38]. For all discrete OT methods, we treat the functional data as point clouds of high dimensional vectors. We can see that FOT successfully transported source sample curves to match target samples. By contrast, GPOT only altered the oscillation of curves but failed to capture the target distribution's multi-modality, while LSOT and DSOT essentially ignored the smoothness of the sampled curves.

For a quantitative comparison, we used the Wasserstein distance to indicate how well the pushforward of source samples match the target samples:

$$L = \min_{\Pi} \frac{1}{n_L} \sum_{l,k} d(T(\mathbf{f}_{1l}), \mathbf{f}_{2k}) \Pi_{lk}. \quad (15)$$

Here, $d(\mathbf{x}, \mathbf{y}) := \|\mathbf{x} - \mathbf{y}\|_2^2$, $\{T(\mathbf{f}_{1i})\}_{i=1}^{n_l}$ and $\{\mathbf{f}_{2i}\}_{i=1}^{n_k}$ are mapped samples and target samples, $T(\cdot)$ is the map given by different methods, n_L is the length of each sample function and Π_{lk} is the probabilistic coupling. The experiments are indicted by $k_{source} \rightarrow k_{target}$, where k is the number of mixture components in the data. More mixture components implies a more complicated data

Method	1 → 1	1 → 2	2 → 1	2 → 2	2 → 3
GPOT	17.560	12.895	15.263	61.561	39.159
LSOT	133.434	94.229	117.832	929.108	663.461
DSOT	6.871	13.226	9.679	46.521	41.009
FOT	2.873	11.982	3.316	44.071	32.547

Table 1: Quantitative comparison on the mixture of sinusoidal functions data. The maps obtained by FOT method achieved the best performance under the Wasserstein distance objective.

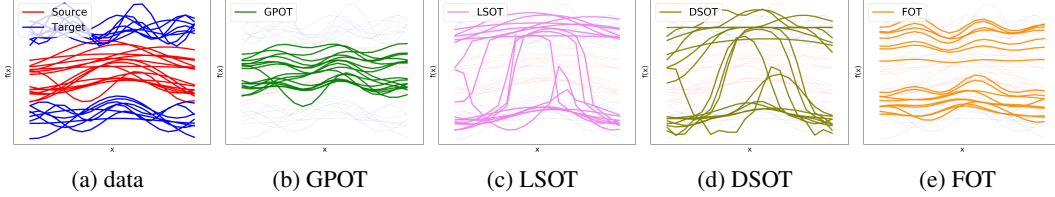


Figure 3: Pushforward results learned by various approaches on mixture of sinusoidal functions data: (a) Sample functions from **source** and **target** domain. The resulting pushforward maps of (b) GPOT [33]; (c) LSOT [26]; and (d) DSOT [38]; and (e) our method FOT.

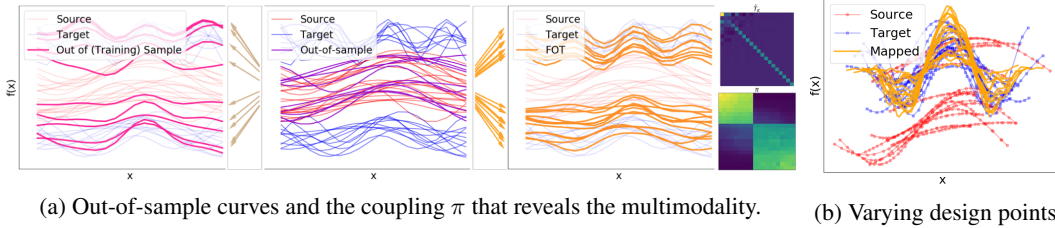


Figure 4: While FOT mapping can transport out-of-sample examples towards a multimodal target. It is also effective when observed curves are evaluated on different design points.

distribution. As demonstrated in Table 1, the pushforward map obtained by FOT performed the best in matching target sample functions quantitatively.

Continuous properties As shown in Fig. 4a, the map learned by FOT does a good job at pushing forward out-of-sample curves that were not observed during training. In addition, the coupling π reveals the multi-modality in the data. Fig. 4b shows FOT is also effective for functional data evaluated at different design points.

5.2 Optimal Transport Domain Adaptation for Robot Arm Multivariate Sequences

Recent advances in robotics include many novel data-driven approaches such as motion prediction [24], human-robot interaction [31], etc [47, 52]. However, generalizing knowledge across different robots, or from one (automated) task to another are considered challenging since data collection in the real world is expensive and time-consuming. A variety of approaches have been developed to tackle these problems, such as domain adaptation [5], transfer learning [50], and so on [46, 13].

Optimal transport domain adaptation We applied our proposed method on an optimal transport based domain adaptation problem (OTDA) [7] for motion prediction by following three steps: 1) learn an optimal transport map, 2) map the observed source samples towards the target domain, and 3) train a motion predictor on the pushforward samples that lie in the target domain. Although it might be possible to discretize and interpolate data to fixed-size vectors, trajectories of robot motion are intrinsically continuous functions of time of various lengths. So in this task, functional OTDA is a natural choice over existing OT map estimation methods for discrete samples.

Datasets The **MIME** Dataset [44] contains 8000+ motions across 20 tasks collected on a two-armed Baxter robot. The **Roboturk** Dataset [34] is collected by a Sawyer robot over 111 hours. As shown in Figure (5a), both robot arms have 7 joints with similar but slightly different configurations, which enable us to present domain adaptation among them. We picked two tasks, *Pouring (left arm)* and *Picking (left arm)*, from MIME dataset and two tasks, (*bins-Bread, pegs-RoundNut*), from Roboturk dataset. We considered each task as an individual domain.

Pushforward of robot motions Our method successfully learns the transport map that pushes forward samples from one task domain to another. The source dataset contains motion records from task *bins-full* from Roboturk dataset while the target includes motion records from task *Pour (left-arm)* in the MIME dataset. We visualize the motion by displaying the robot joint angles sequences in a

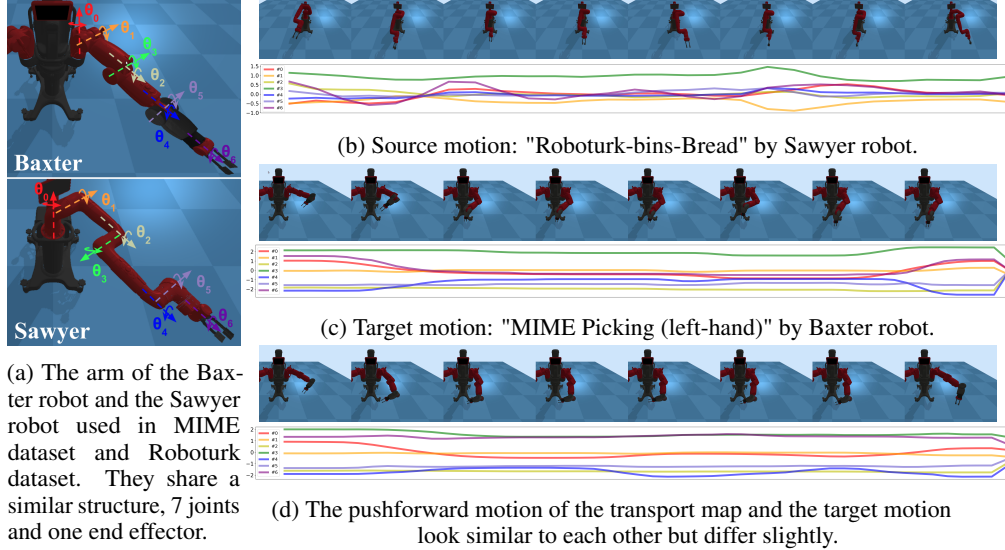


Figure 5: Pushforward of robot arm motions: a motion is visualized as image clips, while the robot-arm joint angles are plotted as a multivariate time series.

Method	LSTM	ANP	RANP	MAML*	TL*	FOT _{LSTM}	FOT _{ANP}	FOT _{RANP}	FOT _{MAML}	FOT _{TL}
R1→M1	2.0217	1.3261	1.9874	0.0307	0.5743	0.0271	0.0963	0.0687	0.0165	0.0277
R1→M2	1.6821	1.0951	1.5681	0.0374	0.7083	0.0414	0.1642	0.1331	0.0191	0.0446
R2→M1	1.3963	0.6642	1.7256	0.0327	0.2491	0.0277	0.0951	0.0696	0.0202	0.0906
R2→M2	1.1952	0.6307	1.3659	0.0477	0.4020	0.0331	0.1620	0.1554	0.0167	0.0406

Table 2: MSE error results of different predictive models. R1: Roboturk-bins-bread, R2: Roboturk-pegs-RoundNut, M1:MIME1-Pour-left, M2: MIME12-Picking-left.

physics-based robot simulation gym [12]. Animated motions can be found here². In Fig. 5, we show image clips of each motion along with a plot of time series of joint angles. We can see from the robot simulation that the pushforward sequence in Fig. 5d matches with the target motion in Fig. 5c while simultaneously preserving certain features of the source motion in Fig. 5b.

Experiment Setup: For the *Robot Arm Motion Prediction* task, a data of length l consists of a set of vectors $S_i \in \mathbb{R}^d$ with associated timestamps t_i . $S = (S_1, t_1), \dots, (S_l, t_l)$ where the time series trajectories are governed by continuous functions of time $f_S(t) : t \in \mathbb{R} \mapsto S \in \mathbb{R}^d$. Since the task is to predict the future l_f points based on the past l_p points, we arrange the data to have the format $X_t = \{(S_{t+1}, t+1), \dots, (S_{t+l_p}, t+l_p)\}$, $Y_t = \{(S_{t+l_p+1}, t+l_p+1), \dots, (S_{t+l_p+l_f}, t+l_p+l_f)\}$.

Our task is learning a predictive model that minimizes the squared prediction error in the target domain $\arg \min_{\theta} \sum_{i=1}^M (F_{\theta}(X_i^t) - Y_i^t)^2$ where Y_i^t is the true label from target domain and $\hat{Y}_i^t = F_{\theta}(X_i^t)$ is the predictive label estimated by a model trained on source domain (X^s, Y^s) and a subset of target domain (X^{tm}, Y^{tm}) .

Methods: We considered 5 baselines to solve this task, including (1) a simple LSTM model using only the source data, (2) the Attentive Neural Process (ANP) [28], which is a deep Bayesian model that learns a predictive distribution (of stochastic processes), (3) the recurrent attentive neural process (RANP) [39], (4) the Model-Agnostic Meta-Learning (MAML) model [13], and (5) a conventional transfer learning (TL) [50] method, where we first trained the model on source domain and then fine-tuned it on target domain. The first three methods can be considered as "zero-shot learning", whereas MAML and transfer learning are considered as "few-shot learning" since a small portion of target data is required for the training.

Results are given in Table 2. Despite the difference of approaches considered, we observe that FOT DA with LSTM, NP, RANP as predictive models outperformed the conventional MAML and TL

²More examples can be found on this website: <https://sites.google.com/view/functional-optimal-transport>.

approaches. Moreover, even MAML and TL can be further boosted by using the mapped samples from FOT.

6 Conclusion

We proposed a method based on subspace approximations of Hilbert-Schmidt operators for learning transport maps that push forward sample functions from one distribution to another. Theoretical guarantees on the existence, uniqueness and consistency of our estimator were provided. Through simulation studies we validated our theory and demonstrated the effectiveness of our method of map approximation and learning from empirical data, by taking into account the functional nature of the data domains. The effectiveness of our approach was further demonstrated in several real-world domain adaptation applications involving complex and realistic robot arm movements. By bridging functional data analysis techniques with the optimal transport formalism we expect to significantly expand the scope of real-world applications in which both functional data and optimal transport viewpoints can play complementary and useful roles toward achieving effective solutions.

Acknowledgments and Disclosure of Funding

We thank Yingchen Ma for providing the ANP and RANP implementations and for helpful discussions on neural processes. Thank you to Rayleigh Lei and Vincenzo Loffredo for valuable discussions and advice on an early version of this paper. Jiacheng Zhu is supported in part by Carnegie Mellon University’s College of Engineering Moonshot Award for Autonomous Technologies for Livability and Sustainability (ATLAS) and by CMU’s Mobility21 National University Transportation Center, which is sponsored by the US Department of Transportation. Aritra Guha is supported by funds from the European Research Council (ERC) under the European Union’s Horizon 2020 research and innovation programme (grant agreement No 856506). Long Nguyen is partially supported by NSF grant DMS-2015361.

References

- [1] David Alvarez-Melis, Stefanie Jegelka, and Tommi S Jaakkola. Towards optimal transport with global invariances. In *The 22nd International Conference on Artificial Intelligence and Statistics*, pages 1870–1879. PMLR, 2019.
- [2] David Alvarez-Melis, Youssef Mroueh, and Tommi Jaakkola. Unsupervised hierarchy matching with optimal transport over hyperbolic spaces. In *International Conference on Artificial Intelligence and Statistics*, pages 1606–1617. PMLR, 2020.
- [3] Martin Arjovsky, Soumith Chintala, and Léon Bottou. Wasserstein gan. *arXiv preprint arXiv:1701.07875*, 2017.
- [4] Bharath Bhushan Damodaran, Benjamin Kellenberger, Rémi Flamary, Devis Tuia, and Nicolas Courty. Deepjdot: Deep joint distribution optimal transport for unsupervised domain adaptation. In *Proceedings of the European Conference on Computer Vision (ECCV)*, pages 447–463, 2018.
- [5] Konstantinos Bousmalis, Alex Irpan, Paul Wohlhart, Yunfei Bai, Matthew Kelcey, Mrinal Kalakrishnan, Laura Downs, Julian Ibarz, Peter Pastor, Kurt Konolige, et al. Using simulation and domain adaptation to improve efficiency of deep robotic grasping. In *2018 IEEE international conference on robotics and automation (ICRA)*, pages 4243–4250. IEEE, 2018.
- [6] Jeffrey Chan, Andrew C Miller, and Emily B Fox. Representing and denoising wearable eeg recordings. *arXiv preprint arXiv:2012.00110*, 2020.
- [7] Nicolas Courty, Rémi Flamary, Devis Tuia, and Alain Rakotomamonjy. Optimal transport for domain adaptation. *IEEE transactions on pattern analysis and machine intelligence*, 39(9):1853–1865, 2016.
- [8] Marco Cuturi. Sinkhorn distances: Lightspeed computation of optimal transport. In *Advances in Neural Information Processing Systems*, 2013.
- [9] Marc Peter Deisenroth, Dieter Fox, and Carl Edward Rasmussen. Gaussian processes for data-efficient learning in robotics and control. *IEEE transactions on pattern analysis and machine intelligence*, 37(2):408–423, 2013.

- [10] Françoise Demengel and Gilbert Demengel. *Functional Spaces for the Theory of Elliptic Partial Differential Equations*. Springer London, 2012.
- [11] Emilien Dupont, Yee Whye Teh, and Arnaud Doucet. Generative models as distributions of functions. *arXiv preprint arXiv:2102.04776*, 2021.
- [12] Zackory Erickson, Vamsee Gangaram, Ariel Kapusta, C. Karen Liu, and Charles C. Kemp. Assistive gym: A physics simulation framework for assistive robotics. *IEEE International Conference on Robotics and Automation (ICRA)*, 2020.
- [13] Chelsea Finn, Pieter Abbeel, and Sergey Levine. Model-agnostic meta-learning for fast adaptation of deep networks. *arXiv preprint arXiv:1703.03400*, 2017.
- [14] Clive AJ Fletcher. Computational galerkin methods. In *Computational galerkin methods*, pages 72–85. Springer, 1984.
- [15] Yaroslav Ganin and Victor Lempitsky. Unsupervised domain adaptation by backpropagation. In *International conference on machine learning*, pages 1180–1189. PMLR, 2015.
- [16] Matthias Gelbrich. On a formula for the 12 wasserstein metric between measures on euclidean and hilbert spaces. *Mathematische Nachrichten*, 147(1):185–203, 1990.
- [17] Aude Genevay, Marco Cuturi, Gabriel Peyré, and Francis Bach. Stochastic optimization for large-scale optimal transport. In *Advances in neural information processing systems*, pages 3440–3448, 2016.
- [18] Edouard Grave, Armand Joulin, and Quentin Berthet. Unsupervised alignment of embeddings with wasserstein procrustes. In *The 22nd International Conference on Artificial Intelligence and Statistics*, pages 1880–1890. PMLR, 2019.
- [19] Nhat Ho, XuanLong Nguyen, Mikhail Yurochkin, Hung Hai Bui, Viet Huynh, and Dinh Phung. Multilevel clustering via wasserstein means. In *International Conference on Machine Learning*, pages 1501–1509. PMLR, 2017.
- [20] Lajos Horváth and Piotr Kokoszka. *Inference for functional data with applications*, volume 200. Springer Science & Business Media, 2012.
- [21] Tailen Hsing and Randall Eubank. *Theoretical foundations of functional data analysis, with an introduction to linear operators*, volume 997. John Wiley & Sons, 2015.
- [22] Chin-Wei Huang, Ricky TQ Chen, Christos Tsirigotis, and Aaron Courville. Convex potential flows: Universal probability distributions with optimal transport and convex optimization. *arXiv preprint arXiv:2012.05942*, 2020.
- [23] Peter J. Huber. Robust estimation of a location parameter. *Annals of Statistics*, 53 (1):73–101, 1964.
- [24] Nikolay Jetchev and Marc Toussaint. Trajectory prediction: learning to map situations to robot trajectories. In *Proceedings of the 26th annual international conference on machine learning*, pages 449–456, 2009.
- [25] Leonid Kantorovitch. On the translocation of masses. *Management Science*, 5(1):1–4, 1958.
- [26] Y Ke. Large-scale optimal transport map estimation using projection pursuit. *NeurIPS 2019*, 2019.
- [27] R.W. Keener. *Theoretical Statistics: Topics for a Core Course*. Springer Texts in Statistics. Springer New York, 2010.
- [28] Hyunjik Kim, Andriy Mnih, Jonathan Schwarz, Marta Garnelo, Ali Eslami, Dan Rosenbaum, Oriol Vinyals, and Yee Whye Teh. Attentive neural processes. *arXiv preprint arXiv:1901.05761*, 2019.
- [29] John Lee, Max Dabagia, Eva L Dyer, and Christopher J Rozell. Hierarchical optimal transport for multimodal distribution alignment. *arXiv preprint arXiv:1906.11768*, 2019.
- [30] Jing Lei. Convergence and concentration of empirical measures under Wasserstein distance in unbounded functional spaces. *Bernoulli*, 26(1):767 – 798, 2020.
- [31] Changliu Liu, Te Tang, Hsien-Chung Lin, Yujiao Cheng, and Masayoshi Tomizuka. Serocs: Safe and efficient robot collaborative systems for next generation intelligent industrial co-robots. *arXiv preprint arXiv:1809.08215*, 2018.

- [32] Ashok Vardhan Makkuva, Amirhossein Taghvaei, Sewoong Oh, and Jason D Lee. Optimal transport mapping via input convex neural networks. *arXiv preprint arXiv:1908.10962*, 2019.
- [33] Anton Mallasto and Aasa Feragen. Learning from uncertain curves: The 2-wasserstein metric for gaussian processes. In *Advances in Neural Information Processing Systems*, pages 5660–5670, 2017.
- [34] Ajay Mandlekar, Yuke Zhu, Animesh Garg, Jonathan Booher, Max Spero, Albert Tung, Julian Gao, John Emmons, Anchit Gupta, Emre Orbay, et al. Roboturk: A crowdsourcing platform for robotic skill learning through imitation. *arXiv preprint arXiv:1811.02790*, 2018.
- [35] Valentina Masarotto, Victor M Panaretos, and Yoav Zemel. Procrustes metrics on covariance operators and optimal transportation of gaussian processes. *Sankhya A*, 81(1):172–213, 2019.
- [36] Cheng Meng, Yuan Ke, Jingyi Zhang, Mengrui Zhang, Wenxuan Zhong, and Ping Ma. Large-scale optimal transport map estimation using projection pursuit. *Advances in Neural Information Processing Systems*, 32:8118–8129, 2019.
- [37] Ardalan Mirshani, Matthew Reimherr, and Aleksandra Slavković. Formal privacy for functional data with gaussian perturbations. In *International Conference on Machine Learning*, pages 4595–4604. PMLR, 2019.
- [38] Michaël Perrot, Nicolas Courty, Rémi Flamary, and Amaury Habrard. Mapping estimation for discrete optimal transport. *Advances in Neural Information Processing Systems*, 29:4197–4205, 2016.
- [39] Shenghao Qin, Jiacheng Zhu, Jimmy Qin, Wenshuo Wang, and Ding Zhao. Recurrent attentive neural process for sequential data. *arXiv preprint arXiv:1910.09323*, 2019.
- [40] Anand Rangarajan, Haili Chui, and Fred L Bookstein. The softassign procrustes matching algorithm. In *Biennial International Conference on Information Processing in Medical Imaging*, pages 29–42. Springer, 1997.
- [41] Filipe Rodrigues, Francisco Pereira, and Bernardete Ribeiro. Gaussian process classification and active learning with multiple annotators. In *International conference on machine learning*, pages 433–441. PMLR, 2014.
- [42] Tim Salimans, Han Zhang, Alec Radford, and Dimitris Metaxas. Improving gans using optimal transport. *arXiv preprint arXiv:1803.05573*, 2018.
- [43] Vivien Seguy, Bharath Bhushan Damodaran, Rémi Flamary, Nicolas Courty, Antoine Rolet, and Mathieu Blondel. Large-scale optimal transport and mapping estimation. *arXiv preprint arXiv:1711.02283*, 2017.
- [44] Pratyusha Sharma, Lekha Mohan, Lerrel Pinto, and Abhinav Gupta. Multiple interactions made easy (mime): Large scale demonstrations data for imitation. *arXiv preprint arXiv:1810.07121*, 2018.
- [45] Asuka Takatsu et al. Wasserstein geometry of gaussian measures. *Osaka Journal of Mathematics*, 48(4):1005–1026, 2011.
- [46] Josh Tobin, Rachel Fong, Alex Ray, Jonas Schneider, Wojciech Zaremba, and Pieter Abbeel. Domain randomization for transferring deep neural networks from simulation to the real world. In *2017 IEEE/RSJ international conference on intelligent robots and systems (IROS)*, pages 23–30. IEEE, 2017.
- [47] Anthony Tompkins, Ransalu Senanayake, and Fabio Ramos. Online domain adaptation for occupancy mapping. *arXiv preprint arXiv:2007.00164*, 2020.
- [48] Cédric Villani. *Optimal transport: old and new*, volume 338. Springer Science & Business Media, 2008.
- [49] Limin Wang. *Karhunen-Loeve expansions and their applications*. PhD thesis, London School of Economics and Political Science (United Kingdom), 2008.
- [50] Karl Weiss, Taghi M Khoshgoftaar, and DingDing Wang. A survey of transfer learning. *Journal of Big data*, 3(1):1–40, 2016.
- [51] Yujia Xie, Minshuo Chen, Haoming Jiang, Tuo Zhao, and Hongyuan Zha. On scalable and efficient computation of large scale optimal transport. *arXiv preprint arXiv:1905.00158*, 2019.

- [52] Mengdi Xu, Wenhao Ding, Jiacheng Zhu, ZUXIN LIU, Baiming Chen, and Ding Zhao. Task-agnostic online reinforcement learning with an infinite mixture of gaussian processes. *Advances in Neural Information Processing Systems*, 33, 2020.
- [53] K. Yosida. *Functional Analysis*. Classics in Mathematics. Springer Berlin Heidelberg, 1995.
- [54] Meng Zhang, Yang Liu, Huanbo Luan, and Maosong Sun. Earth mover’s distance minimization for unsupervised bilingual lexicon induction. In *Proceedings of the 2017 Conference on Empirical Methods in Natural Language Processing*, pages 1934–1945, 2017.
- [55] Huaiyu Zhu, Christopher KI Williams, Richard Rohwer, and Michal Morciniec. Gaussian regression and optimal finite dimensional linear models. 1997.

A Proofs

Fix Borel probability measures μ on H_1 and ν on H_2 . We define the cost function (without regularization term) $\Phi(T) := W_2(T\#\mu, \nu)$ for $T \in \mathcal{B}_{HS}(H_1, H_2)$. For the ease of notation, as in the main text we write n for (n_1, n_2) , K for (K_1, K_2) , \mathcal{B}_{HS} for $\mathcal{B}_{HS}(H_1, H_2)$ and B_K for its restriction on the space spanned by the first $K_1 \times K_2$ basis operators. $\|\cdot\|$ is used to denote the Hilbert-Schmidt norm on operators.

In this section we often deal with convergence of a sequence with multiple indices. Specifically, we say a tuple $m = (m_1, \dots, m_p) \rightarrow \infty$ when $m_1 \rightarrow \infty, \dots, m_p \rightarrow \infty$. By saying that a sequence $F(m_1, m_2, \dots, m_p)$ of index $m = (m_1, \dots, m_p)$ converge to a number a as $m \rightarrow \infty$, it is meant that for all $\epsilon > 0$, there exists M_1, \dots, M_p such that for all $m_1 > M_1, \dots, m_p > M_p$, we have

$$|F(m_1, \dots, m_p) - a| < \epsilon. \quad (16)$$

We write $(m_1, m_2, \dots, m_p) > (m'_1, m'_2, \dots, m'_p)$ if $m_1 > m'_1, \dots, m_p > m'_p$.

We say a function $f(T)$ is *coercive* if

$$\lim_{\|T\| \rightarrow \infty} f(T) = \infty, \quad (17)$$

and it is (weakly) *lower semi-continuous* if

$$f(T_0) \leq \liminf_{k \rightarrow \infty} f(T_k), \quad (18)$$

for all sequences T_k (weakly) converging to T_0 . Further details on convergence in a strong and weak sense in Hilbert spaces can be found in standard texts on functional analysis, e.g., [53].

Now we are going to prove the results presented in Section 3 of the main text. For ease of the readers, we recall all statements before proving them.

Existence and uniqueness First, we verify some properties of objective function J .

Lemma 2. *The following statements hold.*

- (i) $W_2(T\#\mu, \nu)$ is a Lipschitz continuous function of $T \in \mathcal{B}_{HS}(H_1, H_2)$, which implies that $J : \mathcal{B}_{HS} \rightarrow \mathbb{R}_+$ is also continuous.
- (ii) J is a strictly convex function.
- (iii) There are constants $C_1, C_2 > 0$ such that $J(T) \leq C_1\|T\|^2 + C_2 \quad \forall T \in \mathcal{B}_{HS}$.
- (iv) $\lim_{\|T\| \rightarrow \infty} J(T) = \infty$.

Proof of Lemma 2. 1. We first show that $\Phi(T)$ is Lipschitz continuous. Indeed, consider any $T_1, T_2 \in \mathcal{B}_{HS}$, by the triangle inequality applied to Wasserstein metric,

$$\begin{aligned} W_2(T_1\#\mu, \nu) - W_2(T_2\#\mu, \nu) &\leq W_2(T_1\#\mu, T_2\#\mu) \\ &= \left(\inf_{\pi \in \Gamma(\mu, \mu)} \int_{H_1 \times H_1} \|T_1 f_1 - T_2 f_2\|^2 d\pi(f_1, f_2) \right)^{1/2} \\ &\leq \left(\int_{H_1 \times H_1} \|T_1 f_1 - T_2 f_2\|^2 d\pi'(f_1, f_2) \right)^{1/2} \\ &= \left(\int_{H_1} \|T_1 f_1 - T_2 f_1\|^2 d\mu(f_1) \right)^{1/2} \\ &\leq \left(\int_{H_1} \|T_1 - T_2\|^2 \|f_1\|^2 d\mu(f_1) \right)^{1/2} \\ &= \|T_1 - T_2\| \left(\int_{H_1} \|f_1\|^2 d\mu(f_1) \right)^{1/2} \\ &= \|T_1 - T_2\| (E_{f \sim \mu} \|f\|^2)^{1/2}, \end{aligned}$$

where π' is the identity coupling. Hence, both $\Phi^2(T)$ and $\eta\|T\|^2$ are continuous, which entails continuity of J as well.

2. If we can prove that $\Phi^2(T)$ is convex with respect to T , then the conclusion is immediate from the strict convexity of $\eta\|T\|^2$. We first observe that $W_2^2(\cdot, \nu)$ is convex, as for any measure ν_1, ν_2 on H_2 and $\lambda \in [0, 1]$, if γ_1 is the optimal coupling of (ν_1, ν) and γ_2 is the optimal coupling of (ν_2, ν) , then $\lambda\gamma_1 + (1-\lambda)\gamma_2$ is a valid coupling of $(\lambda\nu_1 + (1-\lambda)\nu_2, \nu)$, which yields

$$\begin{aligned} W_2^2(\lambda\nu_1 + (1-\lambda)\nu_2, \nu) &\leq \int_{H_1 \times H_2} \|f - g\|_{H_2}^2 d(\lambda\gamma_1 + (1-\lambda)\gamma_2)(f, g) \\ &= \lambda W_2^2(\nu_1, \nu) + (1-\lambda)W_2^2(\nu_2, \nu). \end{aligned}$$

Now the convexity of $\Phi^2(T)$ follows as for any $T_1, T_2 \in \mathcal{B}_{HS}$, $\lambda \in [0, 1]$,

$$\begin{aligned} W_2^2(((1-\lambda)T_1 + \lambda T_2)\#\mu, \nu) &= W_2^2((1-\lambda)(T_1\#\mu) + \lambda(T_2\#\mu), \nu) \\ &\leq (1-\lambda)W_2^2(T_1\#\mu, \nu) + \lambda W_2^2(T_2\#\mu, \nu). \end{aligned}$$

3. This can be proved by an application of Cauchy-Schwarz inequality and the fact that the operator norm is bounded above by the Hilbert-Schmidt norm. Let π be any coupling of μ and ν ,

$$\begin{aligned} J(T) &= W_2^2(T\#\mu, \nu) + \eta\|T\|^2 \\ &\leq \int_{H_1 \times H_2} \|Tf_1 - f_2\|^2 d\pi(f_1, f_2) + \eta\|T\|^2 \\ &\leq 2 \int_{H_1 \times H_2} (\|Tf_1\|^2 + \|f_2\|^2) d\pi(f_1, f_2) + \eta\|T\|^2 \\ &\leq 2 \left(\|T\|^2 \int_{H_1} \|f_1\|^2 d\mu(f_1) + \int_{H_2} \|f_2\|^2 d\mu(f_2) \right) + \eta\|T\|^2 \\ &= C_1\|T\|^2 + C_2, \end{aligned}$$

for all $T \in B$, where $C_1 = 2E_{f_1 \sim \mu} \|f_1\|_{H_1}^2 d\mu(f) + \eta$, $C_2 = 2E_{f_2 \sim \nu} \|f_2\|_{H_2}^2 d\nu(f)$.

4. This follows from the fact that $\Phi^2(T) \geq 0$ for all T and $\eta\|T\|^2$ is coercive. □

We are ready to establish existence and the uniqueness of minimizer of J . The technique being used is well-known in the theory of calculus of variations (e.g., cf. Theorem 5.25. in [10]).

Theorem 2. *There exists a unique minimizer T_0 for the problem (6).*

Proof of Theorem 2. As $J(T) \geq 0$ and is finite for all T , there exist $L_0 = \inf_{T \in \mathcal{B}_{HS}} J(T) \in [0, \infty)$. Consider any sequence $(T_k)_{k=1}^\infty$ such that $J(T_k) \rightarrow L_0$. We see that this sequence is bounded, as otherwise, there exists a subsequence $(T_{k_h})_{h=1}^\infty$ such that $\|T_{k_h}\| \rightarrow \infty$. But this means $L_0 = \lim J(T_{k_h}) = \infty$ (due to the coercivity), which is a contradiction. Now, because (T_k) is bounded, by Banach-Alaoglu theorem, there exists a subsequence $(T_{k_p})_{p=1}^\infty$ converges weakly to some T_0 . Besides, J is convex and (strongly) continuous. Recall a theorem of Mazur's, which states that a convex, closed subset of a Banach space (Hilbert space in our case) is weakly closed (cf. [53]). As a consequence, function J must be weakly lower semicontinuous. Thus,

$$J(T_0) \leq \liminf_{p \rightarrow \infty} J(T_{k_p}) = L_0. \quad (19)$$

Therefore the infimum of J is attained at some T_0 . The uniqueness of T_0 follows from the strict convexity of J . □

Approximation analysis Next, we proceed to analyze the convergence of the minimizers of finite dimensional approximations to the original problem (6). The proof is valid thanks to the presence of the regularization term $\eta\|T\|^2$.

Lemma 3. *There exists a unique minimizer T_K of J in B_K for each K . Moreover, $T_K \rightarrow T_0$ as $K_1, K_2 \rightarrow \infty$.*

Proof of Lemma 3. Similar to the proof above, for every $K = (K_1, K_2)$ there exists uniquely a minimizer T_K for J on B_K as B_K is closed and convex. Denote $T_{0,K}$ the projection of T_0 to B_K . As $K \rightarrow \infty$, we have $T_{0,K} \rightarrow T_0$, which yields $J(T_{0,K}) \rightarrow J(T_0)$. From the definition of minimizers, we have

$$J(T_{0,K}) \geq J(T_K) \geq J(T_0), \quad \forall K. \quad (20)$$

Now let $K \rightarrow \infty$, we have $\lim_{K \rightarrow \infty} J(T_K) = J(T_0)$ thanks to the Sandwich rule. Since J is convex,

$$J(T_0) + J(T_K) \geq 2J\left(\frac{1}{2}(T_0 + T_K)\right), \quad (21)$$

passing this through the limit, we also have

$$\lim_{K \rightarrow \infty} J\left(\frac{1}{2}(T_0 + T_K)\right) = J(T_0). \quad (22)$$

Now using the parallelogram rule,

$$\begin{aligned} \frac{\eta}{2}\|T_K - T_0\|^2 &= \eta \left(\|T_K\|^2 + \|T_0\|^2 - 2 \left\| \frac{1}{2}(T_0 + T_K) \right\|^2 \right) \\ &= \left(J(T_K) + J(T_0) - 2J\left(\frac{1}{2}(T_0 + T_K)\right) \right) \\ &\quad - \left(\Phi^2(T_K) + \Phi^2(T_0) - 2\Phi^2\left(\frac{1}{2}(T_0 + T_K)\right) \right) \\ &\leq \left(J(T_K) + J(T_0) - 2J\left(\frac{1}{2}(T_0 + T_K)\right) \right), \end{aligned}$$

as Φ^2 is convex. Let $K \rightarrow \infty$, we have the last expression goes to 0. Hence, $\|T_K - T_0\| \rightarrow 0$. \square

What is remarkable in the proof above is that it works for any sequence $(T_m)_{m=1}^\infty$: whenever we have $J(T_m) \rightarrow J(T_0)$ then we must have $T_m \rightarrow T_0$.

Uniform convergence and consistency analysis Now we turn our discussion to the convergence of empirical minimizers. Using the technique above, there exists uniquely minimizer $\hat{T}_{K,n}$ for \hat{J}_n over B_K . We want to prove that $\hat{T}_{K,n} \xrightarrow{P} T_K$ uniformly in K in a suitable sense and then combine with the result above to have the convergence of $\hat{T}_{K,n}$ to T_0 . A standard technique in the analysis of M-estimator is to establish uniform convergence of \hat{J}_n to J in the space of T [27]. Note that the spaces \mathcal{B}_{HS} and all B_K 's are not bounded, so care must be taken to show that $(\hat{T}_{K,n})_{K,n}$ will eventually reside in a bounded subset and then uniform convergence is attained in that subset. The following auxiliary result presents that idea.

Lemma 4. 1. For any fixed C_0 ,

$$\sup_{\|T\| \leq C_0} |\hat{J}_n(T) - J(T)| \xrightarrow{P} 0 \quad (n \rightarrow \infty). \quad (23)$$

2. Let $\hat{T}_{K,n}$ be the unique minimizer of \hat{J}_n over B_K . There exists a constant D such that $P(\sup_K \|\hat{T}_{K,n}\| < D) \rightarrow 1$ as $n \rightarrow \infty$.

Proof. 1. The proof proceeds in a few small steps.

Step 1. We will utilize a recent result on sample complexity theory of Wasserstein distances on function spaces [30]. This theory allows us to find the convergence rate of $EW_2(\hat{\mu}_{n_1}, \mu), EW_2(\hat{\nu}_{n_2}, \nu)$ to 0. By triangle inequality of Wasserstein distances,

$$\begin{aligned} |W_2(T \# \mu, \nu) - W_2(T \# \hat{\mu}_{n_1}, \hat{\nu}_{n_2})| &\leq W_2(T \# \hat{\mu}_{n_1}, T \# \mu) + W_2(\hat{\nu}_{n_2}, \nu) \\ &\leq \|T\|_{op} W_2(\hat{\mu}_{n_1}, \mu) + W_2(\hat{\nu}_{n_2}, \nu). \end{aligned}$$

Therefore,

$$\sup_{\|T\| \leq C_0} |\hat{\Phi}_n(T) - \Phi(T)| \leq C_0 W_2(\hat{\mu}_{n_1}, \mu) + W_2(\hat{\nu}_{n_2}, \nu) \quad (24)$$

Let $r_1(n_1) = E[W_2(\hat{\mu}_{n_1}, \mu)]$ and $r_2(n_2) = E[W_2(\hat{\nu}_{n_2}, \nu)]$. The rates of $r_1(n_1), r_2(n_2) \rightarrow 0$ depend on the decaying rate of Karhunen-Loeve expansions' eigenvalues of μ and ν [30], which exist thanks to our assumption (7). Write $\hat{\Phi}_n(T) := W_2(T \# \hat{\mu}_{n_1}, \hat{\nu}_{n_2})$ for $T \in \mathcal{B}_{HS}$. Then,

$$E \sup_{\|T\| \leq C_0} |\hat{\Phi}_n(T) - \Phi(T)| \leq C_0 r_1(n_1) + r_2(n_2) \rightarrow 0 \quad (n_1, n_2 \rightarrow \infty). \quad (25)$$

As L_1 convergence implies convergence in probability, we have

$$\sup_{\|T\| \leq C_0} |\hat{\Phi}_n(T) - \Phi(T)| \xrightarrow{P} 0, \quad (26)$$

which means for all $\epsilon > 0$,

$$P \left(\sup_{\|T\| \leq C_0} |\hat{\Phi}_n(T) - \Phi(T)| < \epsilon \right) \rightarrow 1, \quad (27)$$

Step 2. Combining $\sup_{\|T\| \leq C_0} |\hat{\Phi}_n(T) - \Phi(T)| < \epsilon$ with the fact that $\Phi^2(T) \leq C_1 \|T\| + C_2$ implies that for all T such that $\|T\| \leq C_0$, we have $\Phi^2(T) \leq C_1 C_0 + C_2 =: C$

$$\begin{aligned} |\hat{J}_n(T) - J(T)| &= |\hat{\Phi}_n^2(T) - \Phi^2(T)| \\ &= |\hat{\Phi}_n(T) - \Phi(T)| |\hat{\Phi}_n(T) + \Phi(T)| \\ &\leq \epsilon(2\sqrt{C} + \epsilon). \end{aligned}$$

Hence

$$P \left(\sup_{\|T\| \leq C_0} |\hat{J}_n(T) - J(T)| < \epsilon(2\sqrt{C} + \epsilon) \right) \geq P \left(\sup_{\|T\| \leq C_0} |\hat{\Phi}_n(T) - \Phi(T)| < \epsilon \right) \rightarrow 1. \quad (28)$$

Noticing that for all $\delta > 0$, there exists an $\epsilon > 0$ such that $\epsilon(2\sqrt{C} + \epsilon) = \delta$, we arrive at the convergence in probability to 0 of $\sup_{\|T\| \leq C_0} |\hat{J}_n(T) - J(T)|$.

2. We also organize the proof in a few steps.

Step 1. Denote $\hat{\Phi}_n(T) = W_2(T \# \hat{\mu}_{n_1}, \hat{\nu}_{n_2})$. We first show that for any fixed C_0 ,

$$\sup_{\|T\| \geq C_0} \frac{|\hat{\Phi}_n(T) - \Phi(T)|}{\|T\|} \xrightarrow{P} 0 \quad (n \rightarrow \infty). \quad (29)$$

Indeed, from (24),

$$\sup_{\|T\| \geq C_0} \frac{|\hat{\Phi}_n(T) - \Phi(T)|}{\|T\|} \leq W_2(\hat{\mu}_{n_1}, \mu) + \frac{W_2(\hat{\nu}_{n_2}, \nu)}{C_0}. \quad (30)$$

Taking the expectation

$$E \sup_{\|T\| \geq C_0} \frac{|\hat{\Phi}_n(T) - \Phi(T)|}{\|T\|} \leq r_1(n_1) + \frac{r_2(n_2)}{C_0}. \quad (31)$$

Hence, $\sup_{\|T\| \geq C_0} \frac{|\hat{\Phi}_n(T) - \Phi(T)|}{\|T\|} \rightarrow 0$ in L_1 , and therefore in probability.

Step 2. For any fixed C_0 and δ ,

$$P \left(\sup_{\|T\| \geq C_0} \frac{|\hat{\Phi}_n(T) - \Phi(T)|}{\|T\|} < \delta \right) \rightarrow 1 \quad (n \rightarrow \infty). \quad (32)$$

The event $\sup_{\|T\| \geq C_0} \frac{|\hat{\Phi}_n(T) - \Phi(T)|}{\|T\|} < \delta$ implies that for all T such that $\|T\| \geq C_0$, we have

$$\hat{J}_n(T) \leq (\Phi(T) + \delta \|T\|)^2 + \eta \|T\|^2 \leq (\sqrt{C_1} \|T\| + C_2 + \delta \|T\|)^2 + \eta \|T\|^2.$$

Now for each K , we can choose a $\tilde{T}_K \in B_K$ such that $\|\tilde{T}_K\| = C_0$. Thus,

$$\begin{aligned} \inf_{T \in B_K} \hat{J}_n(T) &\leq \hat{J}_n(\tilde{T}_K) \leq (\sqrt{C_1 \|\tilde{T}_K\|^2 + C_2 + \delta \|\tilde{T}_K\|})^2 + \eta \|\tilde{T}_K\|^2 \\ &= (\sqrt{C_1 C_0^2 + C_2 + \delta C_0})^2 + \eta C_0^2 =: C, \end{aligned}$$

which is a constant.

On the other hand, choose $D = \sqrt{C/\eta}$, we have for all T such that $\|T\| > D$

$$\hat{J}_n(T) \geq \eta \|T\|^2 > C, \quad (33)$$

which means $\inf_{T \in B_K: \|T\| > D} \hat{\Phi}_n(T) > C$ for all K .

Combining two facts above, we have $\hat{T}_{K,n} \leq D$ for all K .

Step 3. It follows from the previous step that

$$P \left(\sup_K |\hat{T}_{K,n}| \leq D \right) \geq P \left(\sup_{\|T\| \geq C_0} \frac{|\hat{\Phi}_n(T) - \Phi(T)|}{\|T\|} < \delta \right), \quad (34)$$

which means this probability also goes to 1 as $n \rightarrow \infty$. □

We are ready to tackle the consistency of our estimation procedure.

Theorem 3. *There exists a unique minimizer $\hat{T}_{K,n}$ of \hat{J}_n over B_K for all n and K . Moreover, $\hat{T}_{K,n} \xrightarrow{P} T_0$ as $K_1, K_2, n_1, n_2 \rightarrow \infty$.*

Proof of Theorem 3. The proof proceeds in several smaller steps.

Step 1. Take any $\epsilon > 0$. As $T_K \rightarrow T_0$ when $K \rightarrow \infty$, there exist $\kappa = (\kappa_1, \kappa_2)$ such that $\|T_K - T_0\| \leq \epsilon$ for all $K_1 > \kappa_1, K_2 > \kappa_2$. Let

$$L_\epsilon = \inf_{T \in B \setminus B(T_0, \epsilon)} J(T), \quad (35)$$

where $B(T, \epsilon)$ is the Hilbert-Schmidt open ball centered at T having radius ϵ . It can be seen that $L_\epsilon > J(T_0)$, as otherwise, there exists a sequence $(T_p)_p \notin B(T, \epsilon)$ such that $J(T_p) \rightarrow J(T_0)$, which implies $T_p \rightarrow T_0$, a contradiction.

Step 2. Let $\delta = L_\epsilon - J(T_0) > 0$. By Lemma 3, we can choose κ large enough so that we also have $|J(T_K) - J(T_0)| < \delta/2 \forall K_1 > \kappa_1, K_2 > \kappa_2$. Let

$$L_{K,\epsilon} = \inf_{B_K \setminus B(T_K, 2\epsilon)} J(T).$$

As $B(T_0, \epsilon) \subset B(T_K, 2\epsilon)$ and $B_K \subset \mathcal{B}_{HS}$, we have

$$L_{K,\epsilon} = \inf_{B_K \setminus B(T_K, 2\epsilon)} J(T) \geq \inf_{T \in \mathcal{B}_{HS} \setminus B(T_0, \epsilon)} J(T) = L_\epsilon. \quad (36)$$

Therefore,

$$L_{K,\epsilon} - J(T_K) \geq L_\epsilon - J(T_0) - \delta/2 = \delta/2. \quad (37)$$

for all $K > \kappa$.

Step 3. Now, if we have

$$\sup_{\|T\| \leq D} |\hat{J}_n(T) - J(T)| \leq \delta/4, \quad \sup_K |\hat{T}_{K,n}| \leq D, \quad (38)$$

where D is a constant as in Lemma 4, then

$$\hat{J}_n(T_K) \leq J(T_K) + \delta/4, \quad (39)$$

and

$$\hat{J}_n(T) \geq J(T) - \delta/4 \geq J(T_K) + \delta/4, \quad (40)$$

for all $\|T\| \leq D$ and $T \in B_K \setminus B(T_K, 2\epsilon)$, where the last inequality is due to Step 2.

Combining with $|\hat{T}_{K,n}| \leq D$, we have $\hat{T}_{K,n}$ must lie inside $B(T_K, 2\epsilon) \cap B_K$ because it is the minimizer of \hat{J}_n over B_K . Hence $\|\hat{T}_{K,n} - T_K\| \leq 2\epsilon$, which deduces that $\|\hat{T}_{K,n} - T_0\| \leq \|\hat{T}_{k,n} - T_K\| + \|T_k - T_0\| \leq 2\epsilon + \epsilon = 3\epsilon$.

Step 4. Continuing from the previous step, for all κ large enough, we have the following inclusive relation of events

$$\left\{ \sup_{\|T\| \leq D} |\hat{J}_n(T) - J(T)| \leq \delta/4 \right\} \cap \left\{ \sup_K |\hat{T}_{K,n}| \leq D \right\} \subset \left\{ \sup_{K > \kappa} \|\hat{T}_{K,n} - T_0\| \leq 3\epsilon \right\} \quad (41)$$

Using the inequality that for any event A, B , $P(A \cap B) \geq P(A) + P(B) - 1$, we obtain

$$P\left(\sup_{K > \kappa} \|\hat{T}_{K,n} - T_K\| \leq 3\epsilon\right) \geq P\left(\sup_{\|T\| \leq D} |\hat{J}_n(T) - J(T)| \leq \delta/4\right) + P\left(\sup_K |\hat{T}_{K,n}| \leq D\right) - 1, \quad (42)$$

which goes to 1 as $n \rightarrow \infty$ due to Lemma 4. Because this is true for all $\epsilon > 0$, we have

$$\hat{T}_{K,n} \xrightarrow{P} T_0, \quad (43)$$

as $K, n \rightarrow \infty$. \square

B Optimization

We propose a coordinate-wise gradient descent approach to optimize the objective $L(\mathbf{\Lambda}, \pi)$ in Eq. (13):

$$\arg \min_{\mathbf{\Lambda} \in \mathbb{R}^{K_2 \times K_1}, \pi \in \hat{\Pi}} \sum_{l,k=1}^{n_1, n_2} C_{lk}(\mathbf{\Lambda}) \pi_{lk} + \eta \|\mathbf{\Lambda}\|_F^2 + \gamma_h \sum_{l,k=1}^{n_1, n_2} \pi_{lk} \log \pi_{lk} + \gamma_p \sum_{l,k=1}^{n_1, n_2} \pi_{lk}^p, \quad (44)$$

where the transportation cost is $C_{lk}(\mathbf{\Lambda}) = \|\mathbf{V}_{2k} \mathbf{\Lambda} \mathbf{U}_{1l}^T \mathbf{y}_{1l} - \mathbf{y}_{2k}\|_2^2$. Solving this objective involves an alternative minimization over $\mathbf{\Lambda}$ and π whereby the first is fixed while the second is minimized, followed by the second fixed and the first minimized. This procedure is repeated until a maximum number of iterations is reached.

Updating $\mathbf{\Lambda}$ with π fixed: Here we want to solve

$$\mathbf{\Lambda}_t = \arg \min_{\mathbf{\Lambda} \in \mathbb{R}^{K_2 \times K_1}} L(\mathbf{\Lambda}, \pi) = \arg \min_{\mathbf{\Lambda} \in \mathbb{R}^{K_2 \times K_1}} \sum_{l,k=1}^{n_1, n_2} C_{lk}(\mathbf{\Lambda}) \pi_{lk} + \eta \|\mathbf{\Lambda}\|_F^2. \quad (45)$$

The minimum is achieved by performing gradient descent minimization algorithm, where the gradient is:

$$\nabla_{\mathbf{\Lambda}} L(\mathbf{\Lambda}, \pi) = 2 \sum_{l=1}^{n_1} \sum_{k=1}^{n_2} \pi_{lk} [(\mathbf{\Lambda} \mathbf{U}_{1l}^T \mathbf{y}_{1l} - \mathbf{V}_{2k}^T \mathbf{y}_{2k}) \mathbf{y}_{1l}^T \mathbf{U}_{1l}] + 2\eta \mathbf{\Lambda}. \quad (46)$$

Updating π with $\mathbf{\Lambda}$ fixed: Now we want to solve

$$\pi_t = \arg \min_{\pi \in \hat{\Pi}} L(\mathbf{\Lambda}, \pi) = \arg \min_{\pi \in \hat{\Pi}} \sum_{l,k=1}^{n_1, n_2} C_{lk}(\mathbf{\Lambda}) \pi_{lk} + \gamma_h \sum_{l,k=1}^{n_1, n_2} \pi_{lk} \log \pi_{lk} + \gamma_p \sum_{l,k=1}^{n_1, n_2} \pi_{lk}^p. \quad (47)$$

To optimize for the probabilistic coupling π , we can consider this as a constrained linear programming problem. The augmented Lagrangian is given as

$$\begin{aligned} \mathcal{L}(\pi, s_{lk}, \lambda^k, \lambda^l, \lambda^{lk}) &= \sum_{l,k=1}^{n_1, n_2} C_{lk} \pi_{lk} + \gamma_h \sum_{l,k=1}^{n_1, n_2} \pi_{lk} \log \pi_{lk} \\ &+ \sum_{k=1}^{n_2} \lambda^k \left(\sum_{l=1}^{n_1} \pi_{lk} - p_k^t \right) + \sum_{l=1}^{n_1} \lambda^l \left(\sum_{k=1}^{n_2} \pi_{lk} - p_l^s \right) + \frac{\rho_k}{2} \left(\sum_{l=1}^{n_1} \pi_{lk} - p_k^t \right)^2 + \frac{\rho_l}{2} \left(\sum_{k=1}^{n_2} \pi_{lk} - p_l^s \right)^2 \\ &+ \sum_{l,k=1}^{n_1, n_2} \lambda^{lk} (\pi_{lk} - s_{lk}) + \sum_{l,k=1}^{n_1, n_2} \frac{\rho_{lk}}{2} (\pi_{lk} - s_{lk})^2. \end{aligned} \quad (48)$$

In the above display, $\lambda^k \in \mathbb{R}^{n_1 \times 1}$, $\lambda^l \in \mathbb{R}^{n_2 \times 1}$, $\lambda^{lk} \in \mathbb{R}^{n_1 \times n_2}$ are Lagrange multipliers, $s_{lk} \in \mathbb{R}^{n_1 \times n_2}$ are the slack variables. The sub-problem is

$$\begin{aligned}
\pi_t, s_{lkt} &= \arg \min_{\pi, s_{lk}} \mathcal{L}(\pi, s_{lk}, \lambda^k, \lambda^l, \lambda^{lk}) \\
\lambda_t^k &= \lambda_{t-1}^k + \rho_k \left(\sum_{l=1}^{n_1} \pi_{lk} - p_k^t \right) \\
\lambda_t^l &= \lambda_{t-1}^l + \rho_l \left(\sum_{k=1}^{n_2} \pi_{lk} - p_l^s \right) \\
\lambda_t^{lk} &= \lambda_{t-1}^{lk} + \rho_{lk} \left(\sum_{l,k=1}^{n_1, n_2} \pi_{lk} - s_{lk} \right).
\end{aligned} \tag{49}$$

In addition, it is worth noting that when $\gamma_p = 0$, the objective (44) reverts to the form of Sinkhorn distance [8], so that we can take advantage of the superior computational complexity brought upon by the Sinkhorn algorithm.

Algorithm 2: Sinkhorn algorithm

Input: Cost matrix $\mathbf{C} \in \mathbb{R}^{N \times n}$, entropy coefficient γ
 $\mathbf{K} \leftarrow \exp(-\mathbf{C}/\gamma)$, $\nu \leftarrow \frac{1}{n}$
while not converged **do**
 $\mu \leftarrow \frac{1}{N} \odot \mathbf{K}\nu$
 $\nu \leftarrow \frac{1}{n} \odot \mathbf{K}^T \mu$
end while
 $\mathbf{\Pi} \leftarrow \text{diag}(\mu) \mathbf{K} \text{diag}(\nu)$
Output: $\mathbf{\Pi}$

C Experiments

C.1 Additional experiments

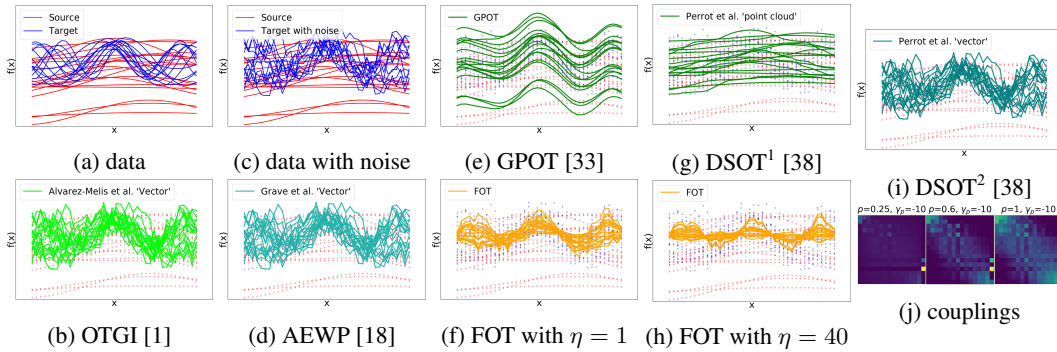


Figure 6: (a),(c): noisy versions as observations. When Perrot’s DSOT [38] (i), Alvarez-Melis’ OTGI [1] (b) and Grave’s AEWV [18] (d) adapt to the noisy data leading to over-fitting, our method (f),(h) performs better in terms of identifying the ground truth. This suggests the effectiveness of treating data as sampled functions (rather than sampled vectors). From (f) and (h) we can see that the parameter η controls the smoothness of the map. Since we could not find the code of method (b) and (d), the results described here come from our own implementation of these methods.

In this part, we show additional experiments with more baseline methods for the same settings considered in section 5.1. Although one can always apply existing OT map estimation methods [1, 38, 18] to functional data by discretizing continuous functions into fixed-dimension vector

measurements, we nevertheless demonstrate this discretization approach fails to exploit the functional properties for most existing OT approaches. We added noncontinuous noise to the target sinusoidal curves and only the pushforward of maps estimated with GPOT[33] and our methods successfully recover the smoothness.

C.2 Experiment details

Hardware: All experiments were implemented with Numpy and PyTorch (matrix computation scaling) using one GTX2080TI GPU and a Linux desktop with 32GB memory.

Synthetic data simulation: We illustrated our approach on a synthetic dataset in which the source and target data samples were generated from a mixture of sinusoidal functions. Each sample $\{y_i(x_i)\}_{i=1}^n$ is a realization evaluated from a (random) function $y_i = A_k \sin(\omega_k x_i + \phi_k) + m_k$ where the amplitude A_k , angular frequency ω_k , phase ϕ_k and translation m_k are random parameters generated from a probability distribution, i.e. $[A_k, \omega_k, \phi_k, m_k] \sim P(\theta_k)$, and θ_k represents the parameter vector associated with a mixture component.

For all simulations, we set the optimization coefficients as $\rho_k = 800 \times \mathbf{1} \in \mathbb{R}^{N \times 1}$, $\rho_l = 800 \times \mathbf{1} \in \mathbb{R}^{n \times 1}$, $\eta = 0.001$, $\gamma_h = 40$, $\gamma_p = -10$, power $p = 3$. The learning rate for updating Λ is $lr_\Lambda = 4e - 4$, the learning rate for updating π_{lk} is $lr_\pi = 1e - 5$. The maximum iteration step is set as $T_{max} = 1000$. We found that our algorithm's performance was not sensitive to varying hyperparameters.

C.3 Karhunen-Loève expansions

Algorithm 1 requires making a choice of basis functions for each Hilbert space in both the source and target domains. In principle, we can take any orthonormal basis for a class of functions of interest. However, a particular choice of orthonormal basis functions may have a substantial impact on the number of basis functions that one ends up using for approximating the support of the distributions (of the source and the target domain), and for the representation of the approximate pushforward map going from one domain to another.

For the current study, we shall exploit the Karhunen-Loève expansion of square-integrable stochastic processes with some specified kernels, which gives us a natural collection of basis functions. Suppose that we are interested in Hilbert spaces of functions defined on a measure space (E, \mathcal{B}, μ) , where E typically is a subset of \mathbb{R}^d . We will first recall Mercer's theorem to see the connection between kernels, integral operators and bases of functions, then present the Karhunen-Loève theorem to link it to stochastic processes and random elements in Hilbert spaces [21]. To serve that purpose, here we only consider continuous, symmetric and non-negative definite kernel, i.e. a function $K : E \times E \rightarrow \mathbb{R}$ being continuous with respect to each variable, having $K(s, t) = K(t, s) \forall s, t \in E$, and for all $n \in \mathbb{N}$, $(\alpha_i)_{i=1}^n \in \mathbb{R}$, $(t_i)_{i=1}^n \in E$,

$$\sum_{i=1}^n \sum_{j=1}^n \alpha_i \alpha_j K(s_i, s_j) \geq 0. \quad (50)$$

If K further satisfies $\int_{E \times E} K(s, t) d\mu(s) d\mu(t) < \infty$, we can define integral operator \mathcal{K} by

$$(\mathcal{K}f)(t) = \int_E K(s, t) f(s) d\mu(s), \quad (51)$$

for all $f \in L^2(E, \mathcal{B}, \mu)$. By Cauchy-Schwarz inequality, we can see that \mathcal{K} maps $L^2(E, \mathcal{B}, \mu)$ to $L^2(E, \mathcal{B}, \mu)$. If $\lambda \in \mathbb{R}$ and $\phi \in L^2(E, \mathcal{B}, \mu)$ satisfy

$$\mathcal{K}\phi = \lambda\phi, \quad (52)$$

then λ is called an eigenvalue of \mathcal{K} and ϕ its corresponding eigenfunction.

Theorem 4 (Mercer's theorem). *Suppose that K is a continuous, symmetric, non-negative definite kernel and \mathcal{K} is its corresponding integral operator; then there exists an orthonormal basis (ϕ_k) of $L^2(E, \mathcal{B}, \mu)$ consisting of eigenfunctions of \mathcal{K} such that its eigenvalues (λ_k) is non-negative. Moreover, K has the following representation*

$$K(s, t) = \sum_{j=1}^{\infty} \lambda_j \phi_j(s) \phi_j(t), \quad (53)$$

where the convergence is absolute and uniform.

Theorem 5 (Karhunen-Loève's theorem). *Let $\{X_t\}_{t \in E}$ be a zero-mean square-integrable stochastic process under a given probability space $(\Omega, \mathcal{U}, \mathcal{P})$ with covariance function being a continuous symmetric non-negative definite kernel K given in the previous theorem. Let $(\lambda_k, \phi_k)_{k=0}^{\infty}$ be the eigenvalue and eigenfunctions of K 's integral operator, then X_t admits the series expansion*

$$X_t = \sum_{k=1}^{\infty} Z_k \phi_k(t), \quad (54)$$

where the convergence is in $L^2(\Omega, \mathcal{U}, \mathcal{P})$, Z_k are zero-mean, uncorrelated random variables satisfying

$$E[Z_i Z_j] = \delta_{ij} \lambda_j \quad \forall i, j \in \mathbb{N}. \quad (55)$$

In the following, we list some Karhunen-Loève bases that have closed forms and can be applied to our algorithm. Detailed derivations can be found in [49, 55].

The Brownian motion. Suppose $E = [0, 1]$ and μ is the Lebesgue measure on E . The Brownian motion is defined by

$$K(s, t) = \min\{s, t\}, \quad \forall s, t \in [0, 1]. \quad (56)$$

The set of eigenvalues and eigenfunctions are given by

$$\lambda_k = \frac{4}{(2k-1)^2 \pi^2}, \quad \phi_k(t) = \sqrt{2} \sin \left[\left(k - \frac{1}{2} \right) \pi t \right], \quad k \geq 1. \quad (57)$$

The Square Exponential Kernel. When $E = \mathbb{R}$ and μ is the Gaussian distribution with mean 0 and covariance σ^2 , we consider the square exponential kernel as follows

$$K(s, t) = \exp(-(s-t)^2/2l^2). \quad (58)$$

We have the set of eigenvalues and eigenfunctions corresponding to K to be

$$\lambda_k = \sqrt{\frac{2a}{A}} B^k, \quad \phi_k(t) = \exp(-(c-a)x^2) H_k(\sqrt{2c}x), \quad k \geq 0, \quad (59)$$

where $H_k(x) = (-1)^k \exp(x^2) \frac{d^k}{dx^k} \exp(-x^2)$ is the k -th order Hermite polynomial, while the constants are defined by

$$a = \frac{1}{4\sigma^2}, \quad b = \frac{1}{2l^2}, \quad c = \sqrt{a^2 + 2ab}, \quad A = a + b + c, \quad B = \frac{b}{A}. \quad (60)$$

Eigenfunction decomposition An alternative way to estimate the eigenfunctions from empirical data is by exploiting Mercer's eigenfunction decomposition. From Mercer's theorem we know a single kernel can be written as a weighted inner product involving a diagonal matrix containing eigenvalues. So a kernel matrix $\mathbf{K} = (K(s_i, s_j))_{i,j=1}^N$ can be written as

$$\mathbf{K} = \sum_{j=1}^{\infty} \lambda_j \phi_j(\mathbf{s}) \phi_j(\mathbf{s})^T, \quad (61)$$

where $\phi_j(\mathbf{s}) = [\phi_j(s_1), \dots, \phi_j(s_n)]^T$. Therefore, we can approximate the eigenfunctions by applying a singular value decomposition to the kernel matrix \mathbf{K} . In addition, the coefficients of eigenvalues can be obtained using the kernel function parameters estimated via Gaussian process regression. For design points $(\mathbf{x}_{1l})_{l=1}^{n_1}$ and $(\mathbf{x}_{2k})_{k=1}^{n_2}$, we can perform GP regression to source and target data respectively to find the optimal kernel function parameters and then

$$\text{SVD}(\mathbf{K}_{1l}) = \mathbf{U}_{1l} \mathbf{D}_{1l} \mathbf{U}_{1l}^T, \quad \text{SVD}(\mathbf{K}_{2k}) = \mathbf{V}_{2k} \mathbf{D}_{2k} \mathbf{V}_{2k}^T \quad (62)$$

thus we can have an empirical estimate for eigenfunctions.

C.4 Optimal transport map of Gaussian processes (GPs)

In Section 5.1, we used the optimal transport map between two Gaussian processes as one of the benchmarks since there exists an explicit expression for the optimal transport map [35].

Optimal transport for GPs. GPs are closely related to *Gaussian measures* on Hilbert spaces [33]. Given probability spaces (X, Σ_X, μ) and (Y, Σ_Y, ν) , if there is a measurable $T : X \mapsto Y$ such that any $A \in \Sigma_Y$ we have $\nu(A) = \mu(T^{-1}(A))$ then we can say ν is a *pushforward* of μ , denoted by $T_{\#}\mu = \nu$. The L^2 -Wasserstein distance between Gaussian measures $N(m, V)$ and $N(n, U)$ is given by [16]

$$W_2(N(m, V), N(n, U))^2 = \|m - n\|^2 + \text{Tr}(V + U - 2(V^{\frac{1}{2}}UV^{\frac{1}{2}})^{\frac{1}{2}}) \quad (63)$$

From lemma 2.4 [45], A *symmetric positive definite matrix* T and its associated linear map \mathcal{T} is defined as

$$T = U^{\frac{1}{2}}(U^{\frac{1}{2}}VU^{\frac{1}{2}})^{-\frac{1}{2}}U^{\frac{1}{2}}, \mathcal{T}(x) = Tx \quad (64)$$

Then, \mathcal{T} pushes $N(V)$ forward to $N(U)$.